Techniques for Measurement of Water Vapor Sorption and Permeation in Polymer Films

K. A. SCHULT and D. R. PAUL*

Department of Chemical Engineering and Center for Polymer Research, The University of Texas at Austin, Austin, Texas 78712

SYNOPSIS

The accurate measurement of water vapor sorption and permeation in polymers is complicated because water has a tendency to adsorb on high energy surfaces, a relatively high heat of vaporization, and a high solubility in most polymers. These issues and the difficulties they cause in the design of sorption and permeation equipment are reviewed. Some new approaches to circumvent these problems are described. Data for bisphenol A polysulfone films are used to illustrate these approaches. © 1996 John Wiley & Sons, Inc.

INTRODUCTION

Water vapor sorption and permeation characteristics of polymers are important for many industries, such as wastewater treatment, gas/air dehydration, pharmaceuticals, and packaging. Accurate measurement of these properties is complicated, however, by the ability of water to hydrogen bond and its high cohesive energy, which create special problems in the design of equipment to determine them. This article reviews these issues and offers another set of approaches to the design and operation of sorption and permeation facilities.

The systems described here for water vapor sorption and permeation measurements were constructed for the study of miscible blends of a relatively hydrophobic polymer with a hydrophilic polymer. The polymer pair employed in the first phase of this work is bisphenol A polysulfone, PSF, and poly(vinyl pyrrolidone), PVP, which are miscible over the entire composition range. Detailed results for this blend system will be reported subsequently. Results for PSF films are used in this article to illustrate the issues involved in the design of equipment for sorption and permeation measurements.

* To whom correspondence should be addressed.

Journal of Applied Polymer Science, Vol. 61, 1865–1876 (1996)
© 1996 John Wiley & Sons, Inc. CCC 0021-8995/96/111865-12

BACKGROUND

It is generally more difficult to make accurate sorption and transport measurements for water vapor than for most other penetrants due to the following characteristic properties of water:

1. a tendency to adsorb on high energy surfaces such as glass or metal;
2. a relatively high heat of vaporization;
3. a low saturation vapor pressure;
4. high solubility in many polymers;
5. a tendency to plasticize polymers, with the level of plasticization being a strong function of activity level; and
6. a tendency to cluster in the polymer at high activities.

To obtain useful data, these properties must be considered, and they necessitate careful design of the experimental apparatus for such measurements.

Factors Affecting Measurement of Sorption Equilibrium and Kinetics

Adsorption

Accurate measurement of both the equilibrium and the kinetics of water vapor sorption can be compromised by water adsorption on high energy surfaces

of certain internal components of the experimental apparatus. Barrie and Machin[1] used an electronic microbalance and concluded that "small but significant amounts of water were sorbed by the balance arm mechanism." They reported that the adsorption was repeatable and nearly independent of temperature. This allowed them to construct "blank" isotherms that were subtracted from the measured isotherms.

Thermal Effects

The high heat of vaporization of water can cause large temperature changes in the polymer during kinetic sorption and desorption experiments. The heat generated when water vapor is sorbed into a polymer will have little thermal effect for a thick sample because the rate of heat dissipation can be much greater than the rate of diffusion. However, for samples with very high surface to volume ratios, such as fibers, the rate of diffusion is often large compared to that of heat dissipation, and this leads to an increase in temperature in the sample. Armstrong and Stannett[2] observed temperature changes of up to 12°C for wool fibers. Diffusion coefficients generally depend rather strongly on temperature. In addition, the increase in sample temperature results in a decrease in the activity just within the sample surface owing to the increase in the equilibrium vapor pressure of water as the sample temperature rises. When this happens, the equilibrium water content just within the surface of the sample decreases. The end result of such an increase in sample temperature is that the diffusion coefficient calculated from gravimetric measurements can be very different than the actual diffusion coefficient.

Armstrong et al.[2,3] experimentally studied the temperature changes that occur during water sorption in wool fibers and ethyl cellulose films, both of which sorb large amounts of water, and developed mathematical methods for determining and correcting for the error in the diffusion coefficient due to these temperature changes. This method only considers the effect that changes in temperature have on the boundary condition at the surface of the fiber or film. It assumes that the diffusion coefficient is a constant and does not take into account how the diffusion coefficient changes with temperature. The magnitude of the temperature effect depends on the following dimensionless parameter,

$$X = \frac{Hb}{L\omega\rho D} \tag{1}$$

where H is the heat transfer coefficient between the sample and its surroundings, b is the half-thickness of the sample, L is the heat of sorption of water vapor, ω is the temperature coefficient of sorption regain (defined below), ρ is the density, and D is the diffusion coefficient of water in the sample.

The heat transfer coefficient can be calculated from unsteady-state heating experiments; Armstrong and Stannett[2] found it to be approximately equal to the value calculated from radiation theory. Because the sample and the surrounding water vapor are at a low pressure, convective heat transfer is small, compared to radiative heat transfer, and can be neglected. This provides a conservative estimate of the heat transfer coefficient. If the change in temperature of the sample is small, the radiative heat transfer coefficient can be approximated as[4]

$$H = 4\sigma T_0^3 \tag{2}$$

where σ is Stefan's constant and T_0 is the temperature of the experiment.

This model assumes a linear relationship between sorption regain (amount of water sorbed per unit mass of polymer) and temperature. The temperature coefficient of regain, ω, mentioned above is defined as follows:

$$W = W_0 - \omega(T - T_0) \tag{3}$$

where W is the equilibrium regain and T is the temperature of the film. Thus, ω is calculated from the slope of plots of the equilibrium regain as a function of temperature relative to a reference temperature; such plots will be illustrated later. Over a broad temperature range the relationship between regain and temperature is usually not linear. Therefore, to use this method in a quantitative way, the change in regain must be kept small so that the change in temperature will be small, ensuring that the local region of the regain versus temperature curve can be approximated as linear.

The heat of sorption of water vapor, ΔH_s, can be calculated from the van't Hoff expression using equilibrium sorption data,

$$\frac{S(T_2)}{S(T_1)} = \exp\left[\frac{-\Delta H_s}{R}\left(\frac{1}{T_2} - \frac{1}{T_1}\right)\right] \tag{4}$$

where S is the solubility coefficient defined as

$$S = \frac{C}{p} \tag{5}$$

and where C is the concentration of water in the sample expressed as milliliters (STP) of water per milliliter of polymer and p is the pressure. The heat of sorption can also be approximated as the heat of condensation of water. A full mathematical treatment is given in the original articles for fibers and for films, respectively.[2,3]

Armstrong et al. developed correction factors for the diffusion coefficient in terms of the dimensionless parameter X (see Table I). In general, when X is greater than 10, the corrections to the diffusion coefficient are small and can often be ignored. When X is less than 10, the corrections are large and cannot be ignored. For very small values of X, the corrections become so large that the experimental results become meaningless.

The temperature rise that occurs during sorption and the error this produces can be minimized by increasing the film thickness; this increases X. Also, use of small activity intervals reduces the amount of water sorbed during the experiment, which in turn reduces the temperature rise in the sample.

Factors Affecting Permeation Measurements

Adsorption

A variety of experimental techniques have been used to study water vapor permeation through polymer films. In many cases, the amount of water that has permeated is determined by monitoring the pressure rise in a downstream receiver volume as a function of time. Typically, the permeate is collected in a glass receiving volume. Water strongly adsorbs on the internal surface of this glass vessel greatly complicating both steady-state and time-lag experiments. Typical steady-state experiments are performed by continuously evacuating the downstream side, while the upstream side of the membrane is exposed to a constant water vapor pressure. When steady state has been reached, the downstream volume is closed and the pressure rise with time is measured. The amount of water adsorbed by the glass increases as the pressure increases; hence, the pressure measured is not a true reflection of the amount of water that permeated through the film. Two studies showed[5,6] that the amount of water sorbed per unit area, Q (mL(STP)/cm^2), at an equilibrium pressure, p_e (mmHg), on washed Pyrex glass at 25°C can be described by

$$Q = 1.73 \times 10^{-4} p_e^{0.422} \tag{6}$$

in the partial pressure range of 0.001–0.03 mmHg. Frank[5] reported that the water adsorption process is relatively fast, with equilibrium being reached within a few minutes.

Water adsorption in this type of apparatus greatly complicates the measurement of the diffusion time lag. Yasuda and Stannett[7] proposed a modified technique that involves placing a diffusion pump between the permeation cell and the downstream receiving volume and prewetting the glass walls with a small amount of water vapor. The diffusion pump maintains a very low pressure at the downstream side of the membrane, which keeps the driving force for transport across the membrane constant, even for low upstream water partial pressures. The diffusion pump also enables the prewetting of the glass walls of the downstream receiving volume because it isolates the downstream side of the membrane from the pressure in the receiving volume. A small amount of water can then be introduced into the

Table I Correction Factors for Diffusion Coefficients due to Thermal Effects[2,3]

	Fibers		Films	
X	$\frac{D \text{ (Corrected)}}{D \text{ (Uncorrected)}}$	Percent Correction	$\frac{D \text{ (Corrected)}}{D \text{ (Uncorrected)}}$	Percent Correction
0.5	6.50	550	5.81	481
1.0	3.65	265	3.35	235
5.0	1.45	45	1.43	43
10.0	1.21	21	1.22	22
50.0	1.04	4	1.047	4.7
100.0	1.015	1.5	1.025	2.5
∞	1.00	0	1.00	0

receiving volume in an attempt to saturate the water adsorption sites on the glass. This technique greatly reduced the error in the measured time lag. However, as Barrie and Machin[8] show, pretreatment of the downstream vessel only reduces, but does not eliminate, the error because the amount of water adsorbed by the glass is a function of the equilibrium pressure of the water vapor. In the course of a permeation run, the pressure in the receiving vessel increases above the pretreatment pressure, and, thus, additional water continues to adsorb onto the glass. Barrie and Machin suggested using an all-metal receiving volume to eliminate these problems.[8]

Other techniques for measuring water vapor permeation through a film have been used that do not rely on measuring the downstream pressure with time. Early water vapor permeation measurements used gravimetric techniques[9] that can be run in one of two ways. Liquid water is placed in a container sealed with a film. The vapor permeates through the film, and the permeability coefficient is calculated from the rate of weight loss of the container. An alternative is to place desiccant in a container covered by a film. The external surface of the film is exposed to a given water vapor activity causing water to permeate through the film and to be adsorbed by the desiccant; the weight gain of the container is measured and used to calculate the permeability coefficient. Edwards and Pickering[10] studied water vapor permeation through rubber and were apparently the first researchers to use these techniques. Wosnessensky and Dubinkow[11] improved on this gravimetric approach by sorbing the permeant onto a desiccant attached to a calibrated quartz spring. The amount of water that permeates through the film can be calculated from the weight gain of the desiccant. This method has the advantage of potentially keeping the downstream vapor pressure nearly zero if the amount of water sorbed is small enough relative to the amount of desiccant used. This technique also reduces the problem of water adsorption onto the glass receiving volume provided water has a greater affinity for the desiccant than glass. Roussis[12] also used a glass receiving vessel and measured the amount of water permeated by monitoring the weight gain of an aluminum calcium silicate zeolite with time. These experiments were done in both time-lag and steady-state modes; however, it was found that as steady state was approached, the zeolite became nearly saturated. This increase in downstream pressure introduces errors in the time lag. Hubbell and colleagues[13] used a stainless steel receiving apparatus as recommended by Barrie and Machin.[8] They swept the downstream side of the film with argon and then measured the amount of water in the argon sweep gas with a hygrometer. They found the water vapor recovery to be greater than 95%, and time lags could be calculated using this method.

High Solubility

In addition to the adsorption problems described above, the high solubility of water in many polymers can lead to errors in permeation measurement if the apparatus is not designed properly. If the downstream volume is not large enough, the magnitude of the downstream pressure rise can cause errors in both the observed permeability coefficient and the time lag. The following discussion is aimed at understanding this problem and describing approaches that can be used to deal with it.

Fick's first law,

$$N_x = -D\frac{\partial C}{\partial x} \tag{7}$$

describes the relationship between the flux, N, of a permeant through a membrane, the concentration gradient, and the diffusion coefficient, D. The experimentally accessible parameter, Q_t, which is the quantity of substance that has permeated through the membrane at time t, can be obtained from the integration of eq. (7),

$$Q_t = \int_0^t N|_{x=l}\,dt = A\int_0^t \left(-D\frac{\partial C}{\partial x}\bigg|_{x=l}\right)dt \tag{8}$$

Fick's second law describes the relationship between the concentration of the penetrant in the membrane as a function of both time and position,

$$\frac{\partial C}{\partial t} = D\frac{\partial^2 C}{\partial x^2} \tag{9}$$

The classical transient permeation solution to these equations requires that the upstream pressure, p_2, and the downstream pressure, p_1, be constant during an experiment. Because the concentration can be related to the pressure by $C = Sp$, a constant pressure also means a constant concentration. In this case, the boundary conditions are

$$\begin{aligned} C = C_1 = Sp_1 \quad & 0 \le x \le l, t < 0 \\ C = C_2 = Sp_2 \quad & x = 0, t \ge 0 \\ C = C_1 = Sp_1 \quad & x = l, t \ge 0 \end{aligned} \tag{10}$$

and the steady-state solution can be expressed as

$$Q_t = \frac{ASD(t - \theta)}{l}(p_2 - p_1) \tag{11}$$

where

$$\theta = \frac{l^2}{6D} \tag{12}$$

When the volume downstream of the film is constant, the pressure p_1 will not remain constant but will rise with time, and this provides a simple way to measure Q_t using the ideal gas law. Under certain conditions the fact that p_1 is a function of time and is not constant causes no significant error and the following pseudo-steady-state relation may be used:

$$\frac{dQ_t}{dt} = \frac{V}{RT}\frac{dp_1}{dt} = \frac{PA}{l}(p_2 - p_1) \tag{13}$$

where A is the membrane area, S is the solubility coefficient, l is the membrane thickness, P is the permeability coefficient, and V is the volume of the downstream receiving vessel.

If p_1 can be maintained at a value negligible to p_2, the result is a linear relationship between p_1 and time, and the permeability can be calculated from the slope of that line.

For time-lag experiments in which the diffusion coefficient is independent of concentration, the time lag, θ, can be related to the diffusion coefficient, D, by eq. (12). If p_1 becomes significant compared to p_2, the driving force for transport will decrease and the downstream pressure rise will no longer be linear with time. If this occurs and the time lag is very small, the steady-state solution can be simplified to

$$\frac{p_2 - p_1(t)}{p_2 - p_1(0)} = e^{-Kt} \tag{14}$$

where $K = PRTA/Vl$.

In this approximation, the permeability can then be determined from the slope of a plot of $\ln(p_2 - p_1(t)/p_2 - p_1(0))$ versus time. If the time lag is not very small, however, this type of analysis fails and an approach that considers diffusion dynamics in the film must be used.

Paul and DiBenedetto[14] analyzed the situation in which the downstream pressure and concentration change with time. After some manipulation, the boundary conditions given by eq. (10) are replaced with

$$\begin{aligned} C = C_{10} = Sp_{10} \quad & 0 \le x \le l, t < 0 \\ C = C_2 = Sp_2 \quad & x = 0, t \ge 0 \\ D\frac{\partial C}{\partial x} + \frac{l}{\eta}\frac{\partial C}{\partial t} = 0 \quad & x = l, t \ge 0 \end{aligned} \tag{15}$$

where p_{10} is the initial pressure on the downstream side of the membrane, and η is given by

$$\eta = \frac{SRTAl}{22{,}414V} \tag{16}$$

The factor 22,414 accounts for the fact that the solubility coefficient is usually expressed as the quantity of gas in milliliters (STP) rather than in moles. The solution to Fick's second law was used to define correction factors for the permeability, solubility, and diffusivity coefficients calculated from the Q_t versus time relation that follows from use of the boundary conditions given in eq. (15) versus those in eq. (10). When η is small enough, these correction factors are given by

$$P_{\text{actual}} = P_{\text{observed}}(1 + 0.69\eta) \tag{17}$$

$$S_{\text{actual}} = S_{\text{observed}}(1 + 0.37\eta) \tag{18}$$

$$D_{\text{actual}} = D_{\text{observed}}(1 + 0.28\eta) \tag{19}$$

As η becomes very small, the correction factors approach unity, and the value of the actual permeability is essentially equal to that of the observed permeability. As η increases, the measured permeability becomes smaller than the actual permeability and must be corrected. For gas permeation experiments, the value for the solubility coefficient, S, is usually small, and it is relatively simple to design permeation systems with η close to zero so that no corrections are required. Because water has a much larger solubility coefficient, typical designs used for gas permeation are not adequate, and so careful attention must be given to the combination of the area, thickness, and receiving volume used to ensure that η will be small.

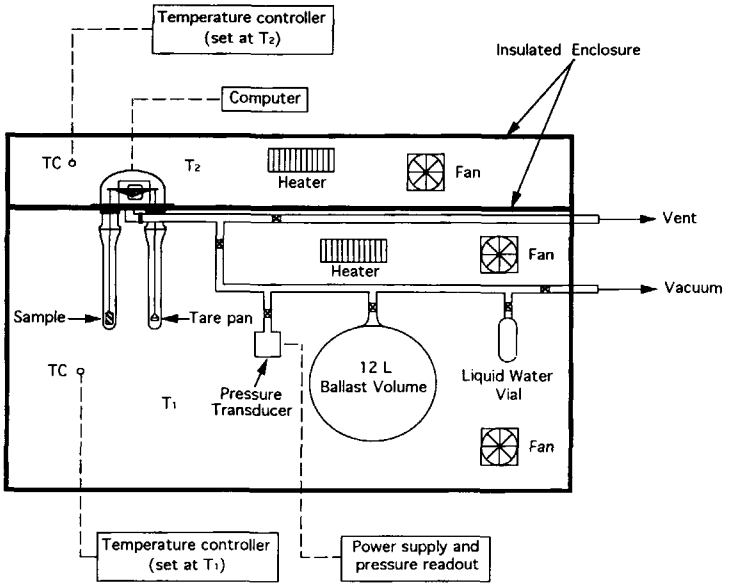

Figure 1 Schematic of sorption apparatus.

EQUIPMENT DESIGN AND MODIFICATION

Materials

Data for films made of pure PSF were used here to illustrate various issues in equipment design. PSF (Udel 1700, Amoco Chemical Co.) is a relatively hydrophobic polymer with a glass transition temperature of 187°C and good mechanical properties. It is used commercially to form membranes for gas separation and ultrafiltration applications.[15]

PSF films were solution cast onto a glass plate using pyridine as the solvent. The glass plate was maintained at 50°C to hasten the evaporation of the solvent, and the film was dried on the glass plate overnight. The film was then placed in a vacuum oven, and the temperature of the oven was gradually increased to just above the glass transition temperature of PSF and held there overnight. Differential scanning calorimetry and thermal gravimetric analysis were used to ensure full removal of the solvent. The films were soaked in liquid water and slowly dried before being used to give them a common history. Films used in sorption experiments were 10–15 mil thick, and those used in permeation experiments were approximately 2–5 mil thick.

Sorption

Apparatus

The sorption apparatus designed for this work (see schematic in Fig. 1) employs a Cahn D-200 digital recording microbalance. The sample is hung from the left balance arm, and the tare is hung from the right arm. This is a null-type instrument that operates by applying an electric current to a torque motor to exactly balance the force created by the sample. The current is then converted to a weight measure and recorded by a computer. The balance is designed for samples with a mass up to 3.5 g and is sensitive to changes in mass of 0.1 μg.

The balance chamber is connected to a liquid water vial, a ballast volume, and a Baratron pressure transducer via a glass manifold. The vial contains liquid water that has been degassed. The Baratron operates over the range of 0–1000 torr and is heated to 100°C to prevent water condensation on the sensor. Before the experiment begins, the balance and sample are isolated from the manifold. The valve to the liquid water vial is then opened until the manifold is at the desired partial pressure of water vapor. At the start of the experiment, the valve between the balance and the manifold is opened, instantly exposing the sample to the desired vapor pressure. Interval sorption experiments were run over sorption activity intervals of 10% at 30, 40, and 50°C. Bouyant forces on the sample were always at least two orders of magnitude less than the gain in weight caused by water sorption.

The apparatus is enclosed in an insulated box, which is divided into two sections. The bottom section is controlled at the desired experimental temperature. The top section only contains the balance weighing mechanism and is maintained at a tem-

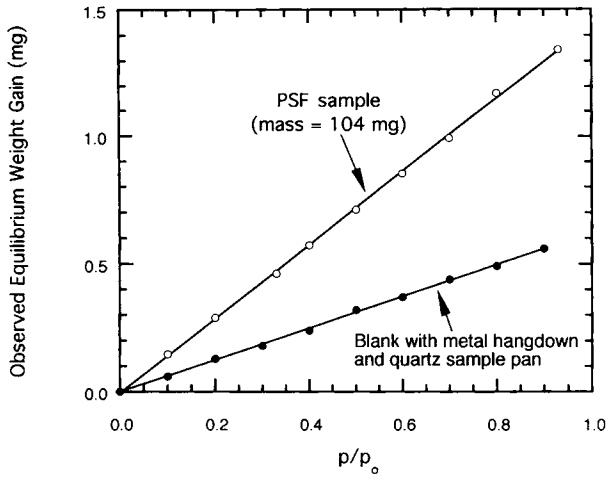

Figure 2 Observed equilibrium sorption isotherms at 40°C for a polysulfone sample and a blank run without a sample, all determined using a nichrome hangdown wire and a quartz sample pan.

perature 2°C higher than the experimental temperature to reduce water condensation and adsorption on the balance arm.

Adsorption Issues

The balance was supplied with nichrome hangdown wires and quartz sample and tare pans; the tare hangdown was only half the length of the sample hangdown. Equilibrium sorption measurements were run at 40°C for a PSF sample with a dry weight of 104 mg. The resulting isotherm is shown in Figure 2. The sample was then removed, and a "blank" isotherm was measured. As can be seen in Figure 2, the net amount of mass recorded without a sample was significant compared to the amount of water recorded when a PSF sample was in the pan; the actual equilibrium sorption isotherm for PSF is approximated by the measured isotherm minus the blank.

The amount of water adsorbed on just the balance arm was found to contribute some to the blank weight gain. This adsorption could be reduced by increasing the temperature of the top section of the insulated box; however, this created a temperature gradient down the hangdown tube, which affected the temperature of the sample. Maintaining the top section 2°C warmer than the bottom section appears to optimize the trade-off between the amount of water adsorption and the temperature gradient along the hangdown tube.

Water adsorption on the quartz sample pans, metal sample pans, and the nichrome wire proved to be significant. The mass gain recorded during this blank run decreased as the lengths of the sample and tare hangdown wires were made more equal. It was found that the water adsorption could be significantly reduced by replacing the nichrome hangdown wires with polyethylene fishing line, lengthening the tare hangdown, eliminating the quartz pan entirely on the sample side, and replacing the quartz pan with a nichrome pan on the tare side. To reduce the blank sorption relative to the sample sorption, the balance was reconfigured for heavier samples. The results of these changes are shown in Figure 3. Equilibrium sorption data were measured for a PSF sample with a mass of 418 mg (see open circles). As a result of these changes, the absolute blank sorption is reduced by approximately 70%, and the blank now contributes only 7% of the total measured weight gain of water in PSF (see open triangles). The actual equilibrium sorption isotherm was approximated by the measured sorption isotherm minus the blank isotherm (see closed circles). There is good agreement between the current data after the changes were made and the data published by Swinyard et al.[16] (see solid line). The blank sorption is reproducible for a given temperature, and it is relatively independent of temperature, as Barrie and Machin reported.[8] Because it is reproducible, it can be reliably subtracted from the apparent sorption values to estimate the actual sorption isotherm.

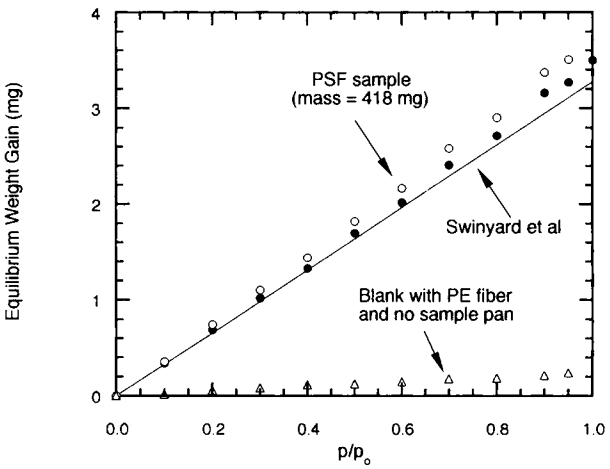

Figure 3 Equilibrium sorption isotherms at 40°C for a PSF sample with a mass of 418 mg and a blank run (open triangles) without a sample, all determined using polyethylene fibers as the hangdown and no sample pan. Open circles represent the observed results. The actual isotherm, approximated as the observed isotherm minus the blank isotherm, is shown by the closed circles. The solid line represents data from Swinyard et al.[16]

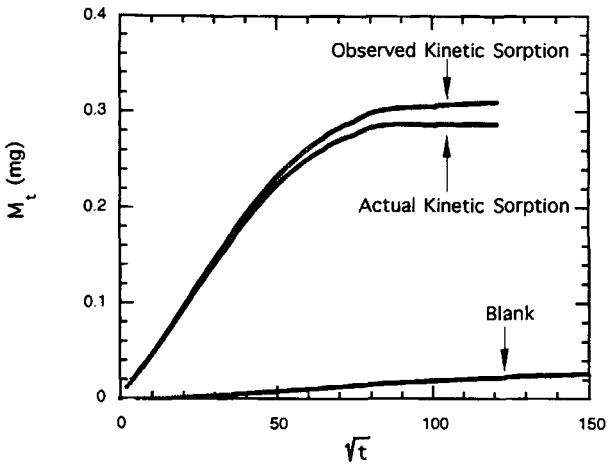

Figure 4 Interval kinetic sorption data for PSF at 30°C over the 0–10% activity interval. The curve obtained by subtracting the blank run from the observed data provides the actual kinetic sorption curve for the PSF sample.

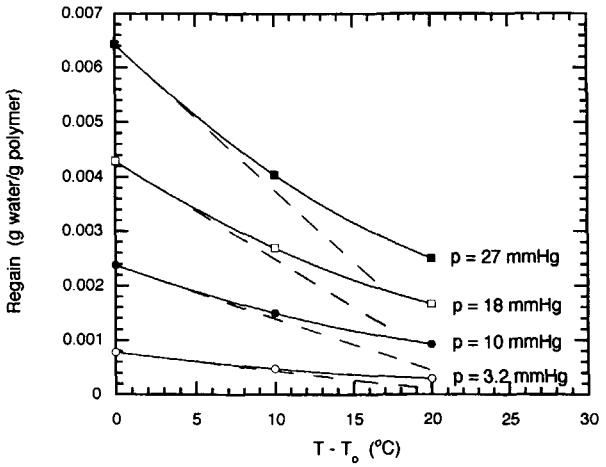

Figure 5 Equilibrium water regain at constant partial pressure as a function of temperature, where T_0 = 30°C. The temperature coefficient of regain for a given pressure is calculated from the initial slope of each curve.

Blank runs of sorption kinetics at 30, 40, and 50°C for 10% activity intervals up to a final activity of 90% were also made. Equations for the blank sorption as a function of time were determined for all activity intervals and temperatures. Figure 4 shows a blank sorption run at 30°C over the activity interval of 0–10%, as well as the observed and actual data for a PSF sample at the same conditions. The "actual" sorption curve is calculated from the observed data minus the blank run.

Thermal Effects

The analysis given by Armstrong and Stannett[2] was used to determine to what extent the diffusion coefficient for PSF calculated from interval sorption/desorption kinetics may be affected by a temperature rise in the film. The half-thickness of the PSF samples used is typically 0.016 cm. Because unsteady-state temperature data were unavailable, the heat transfer coefficient was estimated from radiation theory, eq. (2) to be 1.51×10^{-4} cal/(cm^2 s °C) at 30°C. The diffusion coefficient at 30°C was determined to be nearly independent of activity at about 5.9×10^{-8} cm^2/s. The heat of sorption was calculated from equilibrium sorption data using the van't Hoff expression and was found to be 539 cal/g.

Figure 5 shows a plot of equilibrium sorption regain versus temperature, T, relative to T_0 = 30°C. The values for ω at each pressure were calculated from the initial slopes of the curves and are given in Table II. For an interval sorption from 0 to 10% activity at 30°C, a maximum temperature rise of 1.5°C for the film was calculated from a heat balance, assuming no heat loss from the film to the surroundings. For temperature changes of this magnitude, the curves in Figure 5 are well approximated by linear relations, which means that the method of Armstrong and Stannett is applicable.[2]

The value for X calculated from the above data is equal to 1860 for PSF films at 30°C. According to Table I, the measured diffusion coefficient does not need to be corrected. Again, this method does not account for the change in the diffusion coefficient with temperature, but this effect should also be minor given the relative rates of diffusion to heat transfer involved. In general, using thick films and keeping the activity interval small minimizes the thermal effects associated with the high heat of sorption of water.

Permeation

Apparatus

The permeation apparatus was adapted from equipment used in our laboratories to measure gas per-

Table II Temperature Coefficient of Regain for PSF at 40°C

p (mmHg)	% Regain at 40°C (g water/g polymer)	ω at 40°C (g/g°C)
3.2	0.08	0.000034
10	0.24	0.000102
18	0.43	0.000185
27	0.64	0.000283

meation and is shown schematically in Figure 6. Upstream of the permeation cell is a liquid water vial, a ballast volume, and a Baratron pressure transducer. The pressure transducer operates over the range of 0–1000 torr and is heated to 100°C to prevent condensation on the sensor. Downstream of the permeation cell is a receiving volume and another Baratron pressure transducer that is operable over the range from 0 to 10 torr and is heated to 45°C. This Baratron is connected to a chart recorder to monitor downstream pressure with time. The equipment is enclosed in an insulated box and is temperature controlled to within ±0.2°C by an Omega temperature controller.

Adsorption Issues

The original downstream receiving volume was made of stainless steel, based on the recommendation of Barrie and Machin,[8] with a total downstream volume of 600 mL. Steady-state permeation experiments were run for PSF films using this configuration. Figure 7 shows the measured steady-state throughput, Q_t, at 40°C for an upstream pressure of 33.1 mmHg as a function of time normalized by the membrane area and thickness [see eq. (11)]. The slope of the curve increases with time when the stainless steel volume is used, and the permeability calculated from

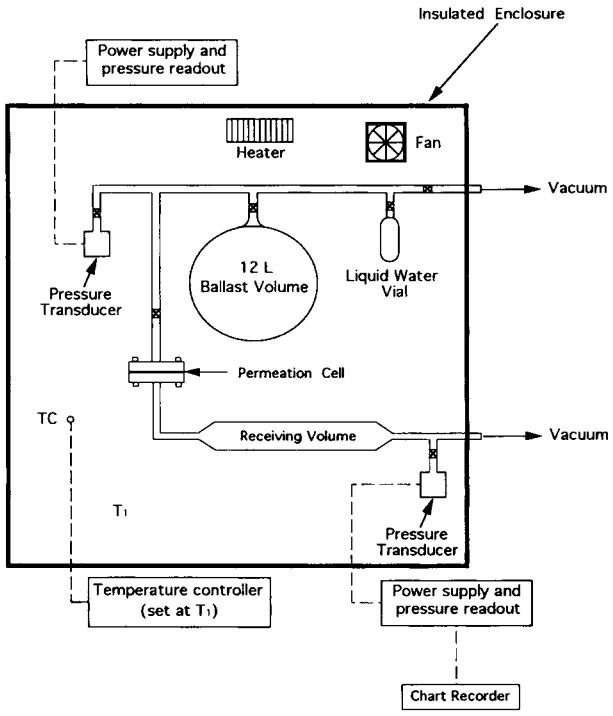

Figure 6 Schematic of permeation apparatus.

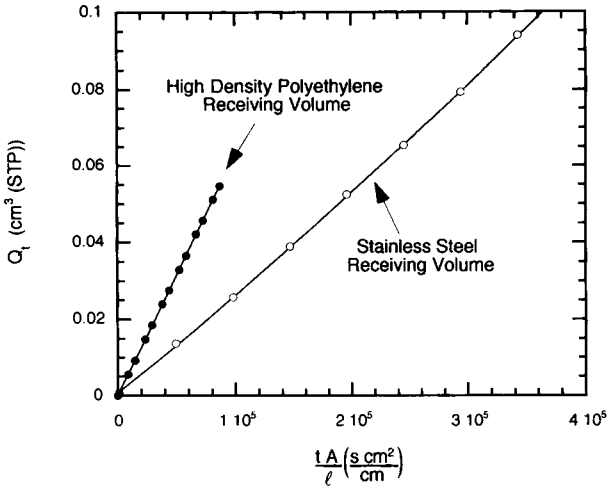

Figure 7 Measured quantity of water permeation at steady state for a PSF film as a function of time normalized by the film area and thickness. The open points were obtained using the stainless steel receiving volume with a sintered metal support disk, and the solid points were obtained using the high density polyethylene receiving volume with a polyethylene support disk.

a tangent to the steepest portion of the curve was much lower than the expected permeability. This suggests that a significant amount of water vapor is adsorbed on the surfaces of the downstream compartment.

Three internal surfaces of the permeation apparatus were identified as the most likely sites for water adsorption: the large receiving volume, the flexible connector tubing, and the sintered metal disk that supports the membrane. To ascertain the amount of adsorption taking place on each surface, the following experiments were performed. The valve located just upstream from the permeation cell was closed, and the film was removed from the permeation cell. The upstream volume was pressurized to the desired water vapor pressure, and the downstream volume was evacuated. Water vapor was then quickly introduced into the downstream volume by letting it flow through the empty permeation cell. The pressure decay was measured, and the amount of water adsorbed was calculated from the pressure decay. Figure 8 shows the results of these experiments.

The first set of experiments was run using a 600-mL total downstream volume that included the large stainless steel receiving volume, the flexible tubing, and the sintered metal disk. As can be seen from Figure 8, a large amount of water adsorption occurred (see the open circles). Next, the large receiv-

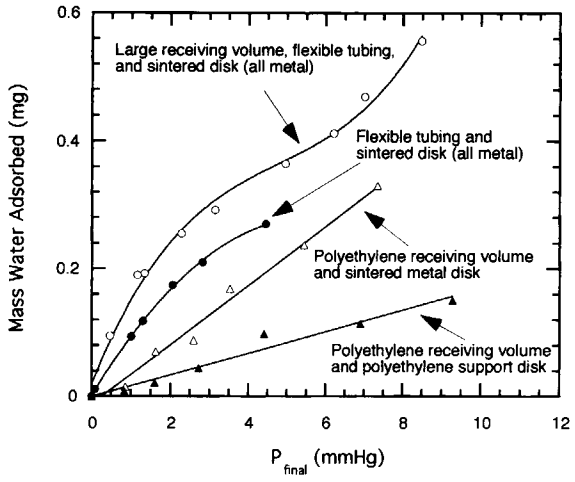

Figure 8 Effect of equipment design changes on the amount of water adsorption onto the downstream surfaces of the permeation apparatus.

ing volume was removed, but the flexible tubing and the sintered metal disk were left in place. The resulting downstream volume was 60 mL. This reduced the amount of water adsorption (see the closed circles). This indicates that some of the originally observed water adsorption occurred on the interior surface of the large receiving vessel, but obviously a large amount of water was adsorbed on the flexible metal tubing and/or the sintered metal support disk. The effects of the flexible tubing and the sintered metal disk could not be separated with the existing equipment design, so it was assumed that both surfaces contributed to the problem. Using these two sets of data, the amount of water adsorbed on the stainless steel receiving volume per unit surface area, Q, was calculated and is shown in Figure 9. The amount of water that adsorbs on glass, according to eq. (6), is also shown in Figure 9. As Barrie and Machin[8] suggested, metal adsorbs less water than glass; however, the amount of adsorption is still significant and must be reduced.

To further reduce the amount of water adsorption, a number of changes were made. First, the large stainless steel volume and flexible tubing were replaced by 3/4-in. i.d. high density polyethylene (HDPE) tubing. The outside of the HDPE tubing was wrapped with metal tape to prevent air from permeating through the tubing into the receiving volume. The total downstream volume after making this change was 605 mL. The effect of this change was determined by experiments like those described above; the results are also shown in Figure 8 (see the open triangles). Clearly, the amount of water adsorption was reduced, but not enough to produce accurate results. Next, the sintered metal support disk was replaced with a porous PE disk, and this resulted in a large decrease in adsorption (see the closed triangles). As can be seen from Figure 8, significant adsorption occurs on the surfaces of the large metal receiving volume, the flexible tubing, and the sintered metal disk; and replacing all of these components with lower energy surfaces was important and effective. All adsorption cannot be eliminated because some stainless steel connections are necessary; however, the amount of adsorption is now small enough to be negligible compared to the amount of water permeating through the membrane. The final result of these design changes is that the downstream volume is now 605 mL, consisting of the PE support disk, the HDPE tubing, the Baratron, and the minimum amount of stainless steel needed to connect these components.

Figure 7 also shows the measured steady-state throughput, Q_t, as a function of time at 40°C for an upstream pressure of 31.5 mmHg after the above changes were implemented. The obtained throughput is linear with time, as would be expected for a steady-state experiment, and the slope of the curve yields the expected permeability. The difference between the two curves shown represents the amount of water adsorbed by the surfaces of the original downstream configuration.

After completing the above changes, time lag experiments were also run for PSF films. At time $t = 0$ the upstream face of the membrane was exposed to the desired partial pressure of water vapor and the downstream pressure was monitored as a function of time. When the downstream pressure approached 1% of the value of the upstream pressure,

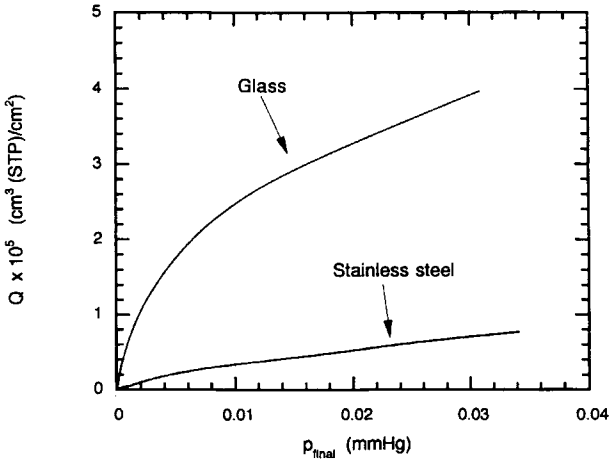

Figure 9 Comparison of water adsorption on glass versus stainless steel at low partial pressures.

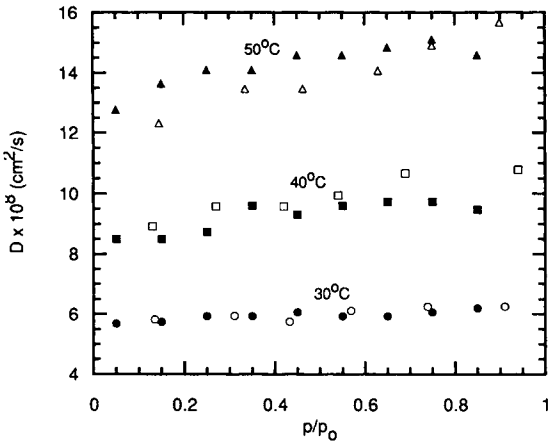

Figure 10 Water vapor diffusion coefficients for polysulfone film (l = 0.0097 cm) at 30, 40, and 50°C as a function of activity. Open points represent data calculated from time-lag experiments and corrected for the effect of the high solubility of water in PSF. Closed points represent data obtained from sorption/desorption kinetics experiments.

the downstream volume was evacuated. The pressure was then allowed to rise again. This procedure was repeated until after steady state was reached. A curve representing the quantity of vapor that permeated through the membrane versus time was constructed, and the time lag was determined in the usual way.[17] The value for the steady-state flux obtained from the time-lag experiments was compared to that obtained from steady-state experiments to ensure that the procedure described above did not produce any errors. As discussed previously, measured time lags must also be corrected using the method of Paul and DiBenedetto.[14] Time lags were measured for PSF at 30, 40, and 50°C. Figure 10 shows the corrected values of these time lags (see open points), and these data compare well to those predicted from sorption/desorption diffusion coefficient data using eq. (12) (see closed points).

Low Vapor Pressure

As mentioned above, the downstream pressure should be negligible compared to the upstream pressure in order to use the steady-state solution for permeation [see eq. (11)]. Because water has a low saturation vapor pressure, it is difficult to maintain this requirement. This problem is most serious when the upstream pressure is low. In the present case the lowest value used is for the experiments at 30°C and 10% relative humidity. At 30°C the saturation vapor pressure of water is 31.8 mmHg. For this case, steady-state data were taken for a downstream pressure range of 0–0.02 mmHg. Yasuda and Stannett[18] recommend keeping the downstream pressure at less than 0.5% of the upstream pressure. Currently, the downstream pressure is kept below 0.6% of the upstream pressure for steady-state experiments and below 1% of the upstream pressure for time-lag experiments.

High Solubility

Initial steady-state permeation experiments were run at 40°C for a PSF film with a thickness of 8.7 mil and a downstream volume of 166 mL. The calculated permeability coefficients from these experiments (see closed circles in Fig. 11) are approximately 30–40% lower than values published by Swinyard et al.[16] (see dashed line). The solubility of water in PSF at 40°C is 2.3 mL (STP)/cmHg mL, which combined with the volume, area, and thickness used leads to $\eta = 0.5$. According to eq. (17) this means a 35% correction to the measured permeability is needed. The values of the permeability coefficient after the correction was made are shown as open circles in Figure 11. While this correction leads to closer agreement with the values given by Swinyard et al.,[16] it is desirable to minimize the correction required by reducing η. The volume was increased to 605 mL, and the film thickness was decreased until the value for η was 0.04. The effect of these changes can be seen in Figure 11. The new

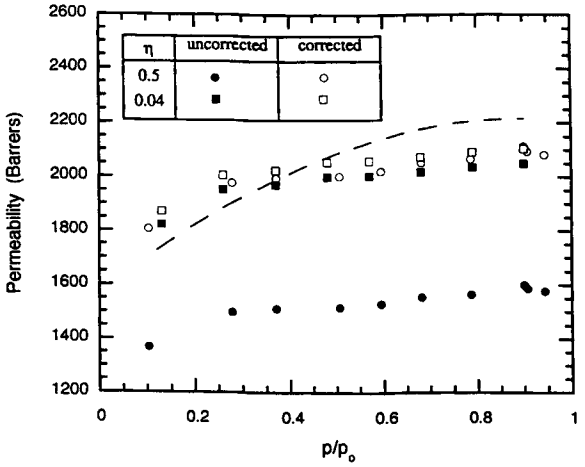

Figure 11 Permeability coefficients for water vapor in polysulfone at 40°C as a function of upstream water vapor activity measured with small and large values of η [see eq. (16)]. Solid points represent uncorrected data, and open points represent corrected data. The dashed line represents data at 40°C from Swinyard et al.[16]

measured permeability coefficients are shown as closed squares, and the corrected permeability coefficients are shown as open squares. Because η is small, the correction for the permeability coefficient is only 3%. The absolute values of the corrected permeability coefficient agree well with the data of Swinyard et al.[16]; however, there is a significant difference in the effect of upstream vapor activity for the two sets of data. The permeability coefficients from Swinyard and colleagues[16] increase approximately 25% over the measured activity range, while the permeability coefficients from this lab increase only 10% over the same activity range. Future articles will address these differences and will present in greater detail the PSF data measured in this lab.

SUMMARY

Water poses many experimental challenges for accurate measurement of its sorption in and permeation through polymer films that can be circumvented by careful equipment design. In the approach used here, critical parts of the measurement apparatus were constructed from materials with low energy or hydrophobic surfaces, such as PE, that greatly reduce the amount of water adsorbed and yield more accurate results for both sorption and permeation measurements. For sorption kinetics experiments, the temperature rise in the film due to the high heat of vaporization of water can be reduced by running experiments over small activity intervals and using thick films. The effect of the high solubility of water in most polymers causes problems in maintaining an effective sink-type boundary condition during permeation measurements, but this can be overcome by increasing the downstream volume, decreasing the membrane area, and decreasing the membrane thickness.

This research was supported by the Separations Research Program at The University of Texas at Austin. K.A.S. acknowledges the Engineering Foundation and the Department of Chemical Engineering at The University of Texas at Austin for fellowship support.

REFERENCES

1. J. A. Barrie and D. Machin, *J. Macromol. Sci. Phys. Ed.*, **3**, 645 (1969).
2. A. A. Armstrong and V. Stannett, *Makromol. Chem.*, **90**, 145 (1966).
3. A. A. Armstrong, J. D. Wellons, and V. Stannett, *Makromol. Chem.*, **95**, 78 (1966).
4. J. Crank, *The Mathematics of Diffusion*, Clarendon Press, Oxford, 1976, p. 368.
5. H. S. Frank, *J. Phys. Chem.*, **33**, 970 (1929).
6. E. P. Barrett and A. W. Gauger, *J. Phys. Chem.*, **37**, 47 (1933).
7. H. Yasuda and V. Stannett, *J. Polym. Sci.*, **57**, 907 (1962).
8. J. A. Barrie and D. Machin, *J. Appl. Polym. Sci.*, **12**, 2633 (1968).
9. R. M. Felder and G. S. Huvard, in *Methods of Experimental Physics*, Vol. 16C, R. A. Fava, Ed., Academic Press, New York, 1980, p. 321.
10. J. D. Edwards and S. F. Pickering, National Bureau of Standards (U.S.), Scientific Paper 387, 1920.
11. S. Wosnessensky and L. M. Dubinkow, *Kolloid-Z.*, **74**, 183 (1936).
12. P. P. Roussis, *Polymer*, **22**, 1058 (1981).
13. W. H. Hubbell, Jr., H. Brandt, and Z. A. Munir, *J. Polym. Sci. Polym. Phys. Ed.*, **13**, 493 (1975).
14. D. R. Paul and A. T. DiBenedetto, *J. Polym. Sci.*, **C10**, 17 (1965).
15. J. E. Harris and R. N. Johnson, in *Mark-Bikales-Overberger-Menges: Encyclopedia of Polymer Science and Engineering*, Vol. 13, 2nd ed., Wiley, New York, 1988, p. 196.
16. B. T. Swinyard, P. S. Sagoo, J. A. Barrie, and R. Ash, *J. Appl. Polym. Sci.*, **41**, 2479 (1990).
17. J. Crank, *The Mathematics of Diffusion*, Clarendon Press, Oxford, U.K., 1976, p. 51.
18. H. Yasuda and V. Stannett, *J. Macromol. Sci. Phys. Ed.*, **3**, 589 (1969).

Received October 23, 1995
Accepted February 20, 1996